Optimization of 3D Printed Liquid Cooled Heat Sink Designs using a Micro-Genetic Algorithm with Bit Array Representation

Connor B. DOKKEN[a] and Brian M. FRONK[a] [b]

[a] School of Mechanical, Industrial and Manufacturing Engineering
Oregon State University
Corvallis, OR 97331 USA

[b]Corresponding author: Phone: +1-541-737-3952 E-mail: brian.fronk@oregonstate.edu

Abstract

The advancement of additive manufacturing enables significantly greater freedom of design compared to conventional techniques. Of significant interest is the potential improvements in the design of cold plates and heat sinks for electronics cooling. Greater design freedom could enable new designs that reduce thermal resistance and hydraulic resistance, enabling the usage of higher power systems while maintaining an equivalent heat sink volume. Additive manufacturing parts are built layer by layer, and can be conceptualized as a bit array in a 2D plane. Therefore, this work explores the feasibility of combining computational fluid dynamics micro-genetic algorithms to produce optimum shapes for liquid cooled heat sinks represented as bit arrays.

A 50 mm × 10 mm area is discretized into a grid space. An initial bit array geometry is developed using a heat flux dependent probability function based on two representative chip power distribution profiles. One distribution is symmetric flux map, and the other uses a non-symmetric map, more representative of a real processor. The performance of generated designs is determined using a commercial computational fluid dynamics code, after which an optimization algorithm is applied. Solution ranking in each generation is based on the system entropy generation rate, which is dependent on the fluid pressure drop and overall heat sink thermal resistance. Crossover, mutation and elitism operations are used to create new generations of designs. Results after one hundred generations are compared with a baseline straight finned cold plate to determine the advantages of designing for an unrestricted manufacturing process. Results indicate that the optimization methods reduced entropy generation rate by 26.4% and 21.7% for the symmetric and non-symmetric power maps, respectively.

Keywords

Heat sink design; genetic algorithms; additive manufacturing; optimization; bit array

NOMENCLATURE

$\dot{m}$	Mass flow rate (kg/s)
ΔP	Pressure drop (Pa)
$\dot{Q}_b$	Power input (W)
ρ	Fluid density (kg/m^3)
$\dot{S}_{gen}$	Entropy generation rate (W/K)
T_∞	Volume average temperature of the working fluid (K)
T_b	Maximum temperature of heating surface (K)

ACRONYMS

AM	Additive Manufacturing
CFD	Computational Fluid Dynamics
CSV	Comma-Separated Values file type
EBM	Electron Beam Melting
GA	Genetic Algorithm
GCI	Grid Convergence Index
LENS	Laser Engineered Net Shaping
PSO	Particle Swarm Optimization
SLM	Selective Laser Melting
SLS	Selective Laser Sintering

1. Introduction

Advances in manufacturing, coupled with improvements in computational power and efficiency, are opening up new opportunities for automating the design and build process of multiple different products. This opportunity is particularly attractive for the creation of new devices for the thermal management of electronics. In this industry, heat densities are rapidly increasing, the physical envelope available for thermal management solutions are decreasing, and the customer base is becoming increasingly fragmented and specialized. One can imagine a future scenario in which a customer specifies the operational requirements of an electronic component and also defines packaging restraints. Power maps of the chipset operating under these specifications could be produced and used as an input to an autonomous design and optimization of a heat sink, which is then fabricated using additive manufacturing as either a prototype or low volume production part with minimal human input. This rapid design/build approach is of increasing importance as the number of high volume customers decreases, and smaller volume customer requirements become increasingly differentiated. A technique to reduce non-reoccurring engineering costs by automating the design and fabrication of a thermal solution for low volume applications could yield large time and monetary savings.

To enable this, the feasibility of combining design optimization techniques with computational thermal/fluid simulations must be explored. Specifically, techniques to minimize computational time while still producing product designs that meet customer requirements must be investigated. Thus, the objectives of this study are to investigate the feasibility of combining micro-genetic algorithms with computational fluid dynamic simulations for the optimization of liquid-cooled heat sinks. The feasibility will be evaluated by considering two different case studies, and evaluating computational resources required and the performance of the micro-genetic algorithm in creating optimal design cases compared to a baseline. In practice, many parameters must be balanced in the optimization process such as cost, size, weight, manufacturability, and performance, among others. In the present study, the optimization criteria will be limited to the overall heat sink thermal resistance and fluid pressure loss, which are combined into a single variable of entropy generation rate. Manufacturability considerations will be limited to the specification of a minimum feature size of 50 μm, which is consistent with the minimum feature that can be resolved by commercial selective laser sintering machines.

2. Prior Work

2.1 Additive Manufacturing

Wong and Hernandez [1] provide an overview of the state of additive manufacturing using, which is of primary interest for heat sink applications. Powder based methods are the most common techniques used in printing, and are utilized in technologies including Selective Laser Sintering (SLS), Electron Beam Melting (EBM), Laser Engineered Net Shaping (LENS) and Prometal. With the exception of LENS, all the systems rely on a base powder bed for fabrication. SLS requires a chamber filled with inert gas to be heated near the melting temperature of the powder. With metals, a binder may be needed, and a laser provides the additional energy input needed to melt the material. The binder is removed post process, often with heating. EBM is similar to SLS, but relies upon a more powerful electron beam to simply melt the material. Prometal also uses the powder bed technique, but purely relies on a liquid binder for processing. The machine applies the binder for each layer, and repeats until the final part is complete. Then the part is finished with cleanup of residual powder, and heat treated to harden the material and binder. Finally, LENS is predominantly used for injection of metal into specific locations. The process uses a laser to melt the material, the material is injected and cools down to form the component. In addition, inkjet based systems are expanding to incorporate metal [2]. In an inkjet system, a jet applies a photopolymer ink to a surface. A UV light is then used to harden the layer. The process repeats until the part is completed. All of these techniques would be viable for production of a heat sink. A key advantage of additive manufacturing is that more of the 2D and 3D design space is available for modification compared to traditional manufacturing technologies such as extrusion, stamping or forming.

An important consideration in using additive manufacturing for heat sink fabrication is the thermal and mechanical properties of the printed part compared to the base material. Bauer *et al.* [3] investigated the manufacture of parts of Haynes® 230 through selective laser melting (SLM). They found a low volume energy density and larger hatch size resulted in a low relative material density at approximately 96.8% of the base metal. With increasing volume energy density and decreasing hatch size, relative density increases to 99.8%. Printed devices had much higher yield strength, slightly higher tensile strength and about equal Young's Modulus to the wrought and cast devices. There is limited study on the thermal conductivity of 3D printed parts versus the base metal. However, the ability to achieve near base metal density of the printed provide some confidence that porosity and the corresponding drop in thermal conductivity is low. The continued evaluation of as-manufactured thermal and mechanical properties will be critical as continued advances are made in the manufacturing field.

2.2. Genetic Algorithms

When considering approaches to optimize parts made using additive manufacturing, it is important to understand how the parts are built. The machines lay material down layer by layer, and the geometry can be defined by a minimum feature size. These are often described by a cubic geometry, which is called a voxel in 3D space. If translated into 2D space, they create pixels, which are also referred to as bits. Topology optimization using genetic algorithms (GA) with bit arrays has been an active area of study in the field of structural mechanics [5–7]. In these studies, the objectives are typically minimization of part mass while maintaining mechanical strength. Genetic algorithms are based on the idea of "survival of the fittest", in that the best solutions are allowed to be "parents" and produce a new generation of solutions (from a number of operators), which repeat the process until some convergence criterion. These algorithms are used to drive a solution based on known best solutions. In the case of a heat sink design, this is difficult, as there are no explicit mathematical results based on individual bit placement. Another option available is particle swarm optimization (PSO), which is similar to GAs, but based on the idea of "particle" position and velocity. The

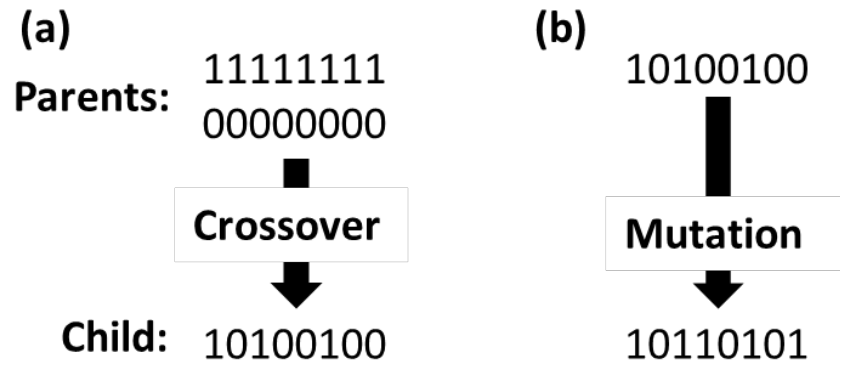

Figure 1: Representation of (a) cross over and (b) mutation operations

idea being that the "particle" has a given velocity based on changing values and the total velocity is influenced by the "swarm" of other particles, which result in dictating a new position each generation. This is unfortunately, difficult and awkward to implement for a discrete problem [10].

When utilizing genetic algorithms, most problems are based on optimizing multiple opposing objectives. Typically, the results are plotted onto an X-Y axis, and form Pareto fronts. With multiple generations, the front should start moving closer to the axis until the system has reached convergence. Ranking the solutions on the front can be done in a few different ways, the most common involve comparing the solutions according to these curves. There are alternative methods, including solution weighting, which use weights to rank each point, in order to determine what will be used to generate the new generation. In a way, this turns the multi-objective optimization into a single-objective problem [11].

Typically, the population size of each generation ranges from around 25 to 100 individuals, and can even be larger [12]. This size is quite limiting for applications requiring intensive numerical analysis to evaluate each population member, as the computational time is significant. To avoid this, some studies have investigated micro-genetic algorithms, which work with populations sizes of around five [13]. To allow an effective greater population variety, an external memory is used that is compared to solutions in the current generation. A few solutions in the current generation are selected (potentially based on ranking), and then a random solution in the memory is chosen. If the generational solution is superior to the one in the memory, that solution is kept in the generation and used to develop the next generation. Additionally, the generational solution replaces the solution in the memory, and is used in any future comparisons. On the other side, if the memory solution is the better solution, it replaces the generation solution and is used to create the succeeding generation.

There are three typical operators that are used to create new generations; crossover, mutation and elitism. Crossover utilizes two parent solutions to create the child, by randomly taking information from the each of the parents and using it to create the child solution. Mutation operators takes a parent, and randomly changes information in it by some percentage to create a child. Often, mutation is combined with crossover operations. Crossover and mutation operators are demonstrated in Figure 1. Finally, elitism brings the parent solution straight through to the new generation with no modification [5].

2.2. Heat Sink Design and Optimization

Ahmed et al. [14] provide a detailed literature review on the state of heat sink optimization considering devices formed with conventional manufacturing techniques including finned and microchannel heat exchangers. However, they do not discuss the potential optimization of unconstrained geometries possible with additive manufacturing, nor do they discuss optimization techniques such as genetic algorithms. Bornoff and Parry [15], explored optimization of a device made with additive techniques by "growing" a heat sink based on an initial plate and uniform heat source in the center of the area. They solved the problem by running a thermal simulation, identifying hot spots and adding material at these locations. Simulations are repeated and additional material is added. Additional growth periods from the base are performed until convergence is reached. They found that the "grown" heat sink showed about a 20% reduction in thermal resistance compared with a baseline extruded heat sink. It is worth noting that the baseline heat sink had much larger fins than the minimum feature size of the "grown" device. To provide a better comparison, they also built an unconstrained finned heat sink to compare. This unconstrained design had no fixed aspect ratio and a minimal feature size the same as the "grown" heat sink. With this comparison, they found that the unconstrained design actually provided 5% lower thermal resistance than the "grown" heat sink.

Gosselin et al. [8] review the utilization of genetic algorithms in heat transfer problems in general, including in system and device design. They review over one hundred and fifty different studies ranging from heat exchangers, thermofluid systems to HVAC&R applications. They report that heat exchanger GA optimization typically relies on analytical solutions, while other thermofluid systems use a combination of 2D heat transfer analysis and CFD approaches. Several authors have used GAs specifically to optimize heat sinks for electronics cooling applications [16–20]. Again, these typically focus on conventionally manufactured devices, and consider things like fin spacing, thickness, height, pitch, etc., as design variables, rather than the bit-array approach considered here. As an example, Wu *et al*. [21] performed research with genetic algorithms to provide optimization for a heat pipe design in a heat sink. They performed a thermal analysis of a commercially available heat sink, which consisted of copper heat pipes carrying coolant (water), embedded in an aluminum block. After analysis of the baseline commercial heat sink was completed, an optimization algorithm technique was applied to improve the design. An initial area was established with an inlet and outlet, as well as a heat source, and the algorithm was allowed to randomly generate paths between the inlet and outlet. Once completed, the designs were evaluated and ranked, and then utilizing genetic algorithms, new generations were created and the process repeated. After a certain amount of iterations were completed, a second stage occurred that performed perturbations on the existing designs, then repeated the genetic algorithm process. The findings showed that the first part of the optimization process resulted in a design that reduced peak temperature from 53.02 °C to 46.10°C, in exchange for an increase of inlet force from 0.56 N to 1.63 N. Similarly, the second part of the optimization process obtained a further reduction in peak temperature to 44.85°C, with an inlet force of 1.3 N. This corresponds to a 15.4% reduction in thermal resistance in exchange for a 132% increase of force (related to pumping power), which may be an acceptable trade-off for some high flux applications. The results show the benefits of optimization processes, but also shows that the results achieved are not always free, in this case with increased internal pressure drop.

Of interest to optimization problems for heat transfer problems are the usage of entropy generation minimization methods. The approach was introduced by Bejan [22]. Starting from general forms of the 1st and 2nd law, an expression that relates pressure drop and thermal resistance to overall entropy generation rate can be derived:

$$\dot{S}_{gen} = \left(\frac{\dot{Q}_b^2}{T_\infty T_b} \right) R_{th} + \frac{\dot{m} \Delta P}{\rho T_\infty} \tag{1}$$

$$R_{th} = \frac{T_b - T_\infty}{\dot{Q}_b} \tag{2}$$

Khan *et al*. [23] applied entropy generation minimization to a pin fin heat sink. The entropy generation rate term used is again similar to that developed by Bejan [22], with substitutions made for the system thermal resistance and pressure drop. Analysis is completed through an iterative method considering different design variables. These variables included the number of pins, pin diameter, pin height and the fluid velocity. The heat sink was limited in area and height, with a set base thickness and a uniform power applied. Two different materials were compared as well, using a plastic composite alongside aluminum. The results show distinct minimum values in entropy generation rate for each of the dependent variables, meaning there is also a distinct optimum for each of the independent variables. However, it is important to recognize that interaction between variables must be taken into account. In the end, they were able to converge on an optimum result between different arrangements and materials, through repeated iteration to minimize entropy.

Genetic algorithms have been extensively used in for optimizing heat exchangers and thermal systems, to the point where their application may be considered “mature” [8]. However, there are relatively few studies in which bit array representations of heat sinks are combined with detailed computational fluid dynamic simulations.

Clearly, genetic algorithms have been widely used in optimization of heat exchangers and thermal systems [8]. Most often, the models evaluated are analytical models that require relatively low computational effort [8]. This allows many solutions to be evaluated across multiple generations in a reasonable time span. The use of additive manufacturing to fabricate heat sinks enables somewhat random, unconventional flow paths effectively built bit-by-bit. For these types of geometries, there are no existing correlations or explicit solutions that can be used to predict the pressure drop and thermal resistance of different designs, requiring more detailed simulation of each solution. This gap in the literature provided the motivation to investigate the use of a micro-genetic algorithm approach for optimizing a bit-array representation of liquid cooled heat sinks. Each potential design was evaluated using a commercial computational fluid dynamics (CFD) program. The two objectives of interest were minimizing fluid pressure drop and overall heat sink thermal resistance. The problem was collapsed into a single-objective optimization problem by using entropy generation rate to rank the solutions. The solution system used a total volume of 52 mm × 50 mm × 12 mm, and a 50 mm × 50 mm × 10 mm of fluid volume space. This size was specified based on a comparable cold plate analysis [9]. The entropy generation rate value is then compared to a traditional finned heat sink design with identical operating conditions.

3. Modeling and Optimization Methodology

Two optimization case studies and a baseline analysis were evaluated. For each optimization case, initial geometries were semi-randomly generated bit-by-bit in an X-Y plane. Then, 3D models were developed and imported into a commercial CFD package where they were meshed and heat transfer and fluid flow parameters simulated. The performance of each solution was ranked and a micro-genetic algorithm approach implemented. The process of micro-genetic algorithm, 3D model, and CFD simulation continued until a set stopping criteria. Details of the initial generation, thermal and fluid simulations and optimization methods are discussed below.

3.1. Initial Design Generation

In the present study, optimization of the heat sink geometry in only the X-Y plane was conducted. The resulting 2D geometries were then "extruded" to form 3D flow structures. Simultaneous 3D optimization in the X-Y and X-Z plane is the ultimate goal of an autonomous design and build scenario. However, this requires significant computational resources that were beyond those available in the present project. Thus, modifications only in the X-Y plane were considered in this first step in exploring heat sink optimization techniques. Optimizing the X-Y plane is consistent with traditional finned heat sinks, which do not have feature variation within the X-Z plane. A demonstrated improvement in performance in only 2D space would suggest further improvements could be realized in future work by considering 3D optimization.

The heat sink volume under consideration is shown in Figure 2. The base device dimensions are set at 52 mm × 50 mm × 12 mm, with an internal fluid volume of 50 mm × 50 mm × 10 mm. These dimensions were chosen to match those of a commercial heat sink [9]. At the inlet and outlet end of the device, a 1 mm thick shroud is extended around the edge, leaving a flow channel the size of the frontal flow area. The shroud extends 5 mm from each end, creating a total device dimension of 52 mm × 60 mm × 12 mm in the simulation. The solutions space is discretized into a bit array with grid spacing of 1 mm, as shown in Figure 3. The 1 mm spacing was choosen as it roughly corresponds to a fin thickness in a conventional heat sink. All analyis for generation of solutions was conducted in MATLAB [24].

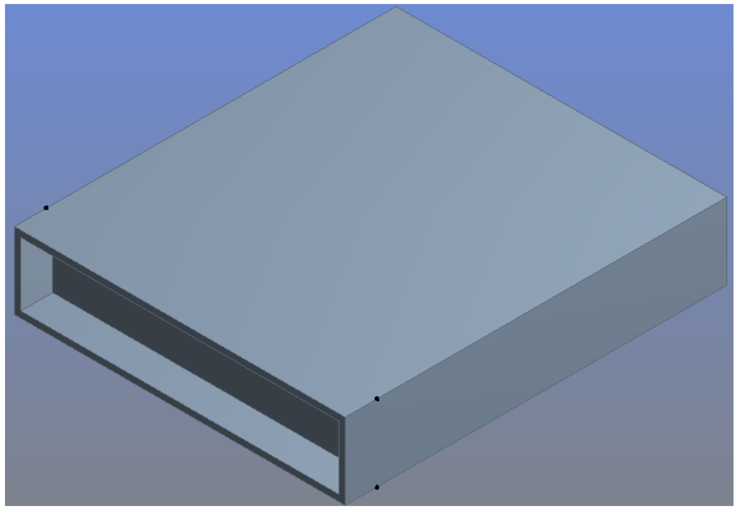

Figure 2: The base of the heat sink before the generated geometry is removed

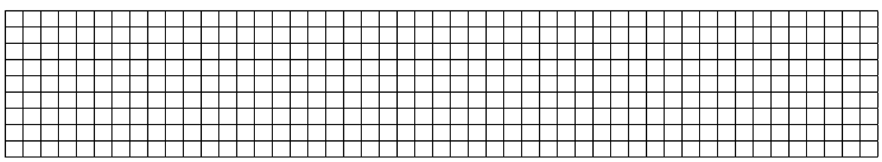

Figure 3: Example of the discretized domain used for geometry generation

Two power maps were used initialize the problem for two different studies. The first analysis utilizes a simple symmetrical power map, with a total area of 50 mm × 50 mm. The center 100 mm^2 is set as the highest power region, with flux of 60 W/cm^2. The second area is 800 mm^2 (minus the center), and has a flux of 40 W/cm^2. The remaining area is 20 W/cm^2. The second analysis utilizes a representative non-symmetrical power map, with a maximum power flux of 20 W/cm^2, and a minimum of 0 W. The total power was 700 W for the symmetric and 218.7 W for the non-symmetric power maps. Both power profiles are shown in the Figure 4 (symmetric) and Figure 5 (non-symmetric).

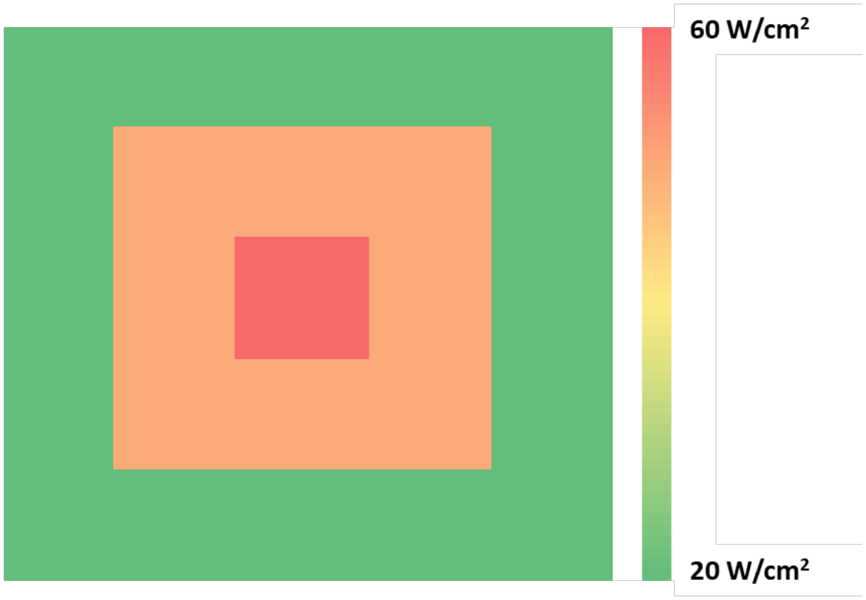

Figure 4: Schematic of symmetric power map

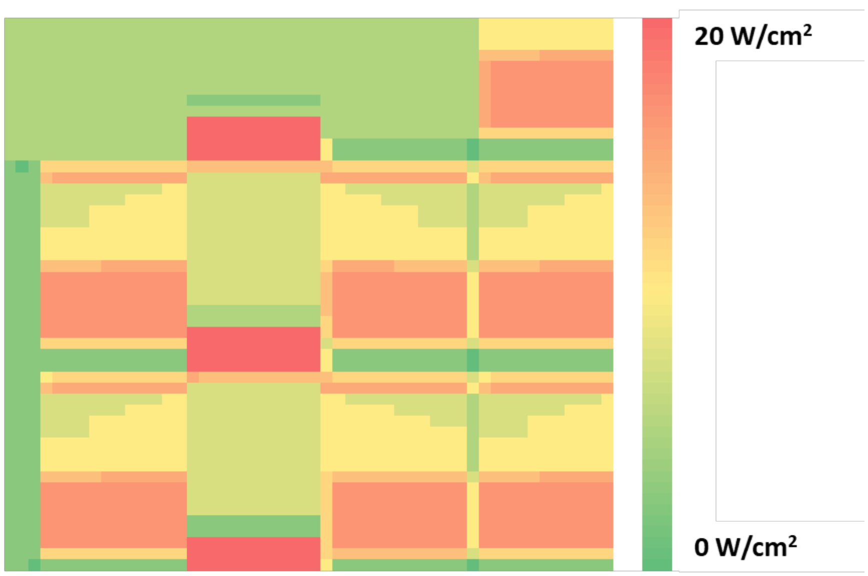

Figure 5: Schematic of non-symmetric power map

Since optimization in a single X-Y plane is considered, the X-Z location with the highest power output for each power profile was used as a worst-case condition. The worst-case power vector was normalized from a range of 0 to 1 based on the maximum power value in the vector. After this, the geometry array is modified to have solid material around the edges (to contain the fluid), creating a 51 × 11 grid. The normalized power is then used to generate the first layer of material. The code goes through the first row bit by bit, and a probability is applied to the bit location to determine if a solid bit is generated. This probability ranged from 15-80% based on the normalized value of the power and a linear relationship. These percentage values were set through trial and error testing, the values chosen are intended to bias the solid bits toward the regions of highest power.

Once the first layer is generated, the rest of the geometry was created based on surrounding material and a 50/50 probability of generation. Power is not directly utilized as it assumed the first layer provides the necessary bias in the structure. Starting directly above the first layer, an analysis at each bit from the left edge to the right in the row was conducted. At each point, it was determined if there is any solid material around the point (including the walls on the side), that a new bit could physically attach to. If there was any material in one of the 8 surrounding cells, the current location is given a 50% chance of generating a solid bit. After this, the next bit location experiences the same operation, and this repeats until the vector is completed. The process repeats with the next layer, starting back on the left edge. After one pass-through in each row is completed, the initial bit array geometry is finalized.

Once the bit array representation of the geometry has been created, it was converted into a physically realistic 2D geometry, and then extruded into 3D. This bit array was converted into a suitable data set using a contour plot function of the array in MATLAB, with representative results shown in Figure 6. Two contour levels are needed to ensure generated curves have realistic geometry. The first initial contour level often leaves bits floating in space, or completely misses material connections. This is overcome by utilizing the second level, in exchange for some dimensional accuracy (approximately a 0.125 mm increase in material thickness, maximum). Finally, the C2xyz script [27] is applied to organize the information from the contour variable into x and y coordinates of the readily extractable groupings. The 2D curve information is then used to create 3D extruded structures in ANSYS, which can be analyzed using CFD.

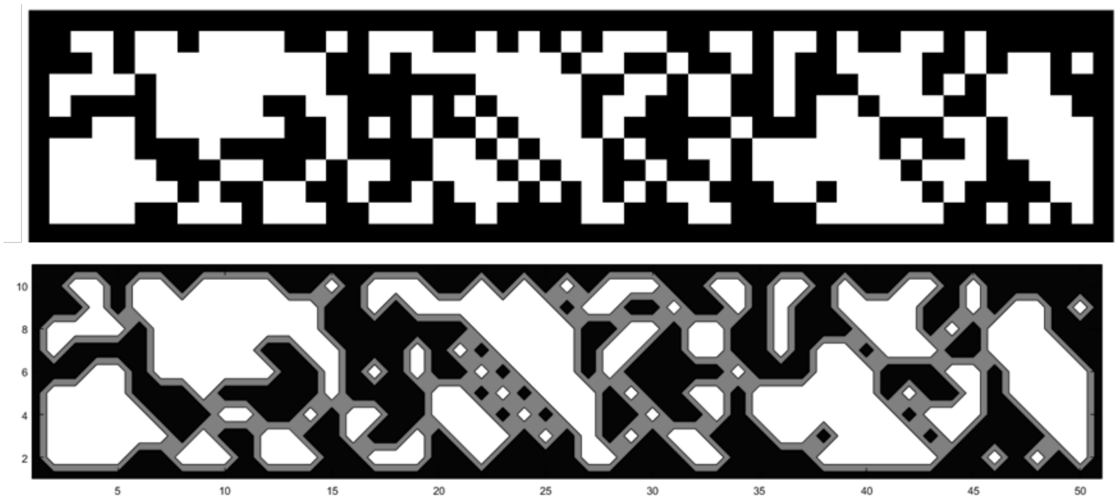

Figure 6: The generated bit image and corresponding contour plot. Note that the black in the contour plot represents the results of the first contour line, while the grey represents the second contour line.

3.2. Thermal and Fluid Simulation Approach

The 3D geometry was meshed using an ANSYS Meshing tool and brought into Fluent [25]. The mesh size was selected after performing a grid convergence index (GCI) study to determine the best balance between the fineness of the grid and analysis speed. Tests were run for both the fluid and solid geometry, with three different grid sizes for each. For the solid, tests were done with a minimum grid size of 0.25, 0.50 and 1.0 mm and analyzed the difference in system temperature to determine convergence. The fluid was analyzed with slightly smaller grid sizes at 0.125, 0.25 and 0.50 mm and total pressure drop is used as a convergence criteria. A grid size of 0.5 mm was selected for each domain, as the percent change in the solution by halving the grid size was less than 1.5%.

The heat sink material used is aluminum with a constant thermal conductivity evaluated at 300 K. The fluid domain is water with constant properties evaluated at 300 K. For all scenarios, water had a low inlet velocity flow of 0.1 m/s at inlet of the frontal cross section to minimize pressure drop and pumping power. The low velocity was also intended to keep the Reynolds number low to simplify simulations. However, during geometry optimization some of the larger internal flow paths resulted in Reynolds numbers that were around 2000, based on local hydraulic diameter. Thus, the Spalart-Allmaras turbulence model was used after considering a trade-off between a laminar only analysis and using the simplified turbulence model. To evaluate the tradeoff in the selected model, a comparison of calculated pressure drop using laminar and Spalart-Allmaras assumptions was conducted for ten different generated geometries. The average difference was less than 3.5%, with a maximum of 5.3%. The potential uncertainty due to the chosen model is addressed in Section 4.4, below. The objective of this study was not necessarily accurate, quantitative results from detailed CFD, but rather investigation of the feasibility of coupling CFD simulation tools with genetic algorithm approaches to produce optimized designs. By conducting all simulations under the same assumptions, uncertainties or inaccuracies introduced would be relative, enabling a qualitative comparison of solutions using the micro-genetic algorithm approach.

Initially, the solid and fluid domains were at a uniform temperature. In the fluid domain, the inlet condition was a uniform velocity at a temperature of 300 K, with no-slip condition enforced at all solid surfaces, and a pressure outlet boundary condition. For the solid domain, a specified heat flux according to the power maps in Figures 4 and 5 were used on the bottom surface, while the top and sides were assumed to be adiabatic. Simulations were run until convergence was achieved with residuals on the order of 10^{-6} to 10^{-5}, typically after 400 iterations. For each solution, energy balances were conducted to ensure agreement within 1%. From the solution, the mixed cup temperature of the fluid domain, maximum surface temperature, fluid pressure drop, and other variables needed to evaluate the rate of entropy generation were evaluated.

3.3 Micro-Genetic Algorithm Approach

The overall optimization process flow is shown schematically in Figure 7. Using the results from the CFD model, the generation solutions from best to worst are ranked based on entropy generation rate. In the initial run, the solutions create the external memory, otherwise the solutions of the generation are compared to the memory. Two numbers between 1 and 25 (or 20 for the non-symmetric) are randomly generated to serve as access numbers to the memory. The associated memory locations are compared to the #2 and #4 ranked solutions via the entropy generation rate. As discussed previously, if the generational

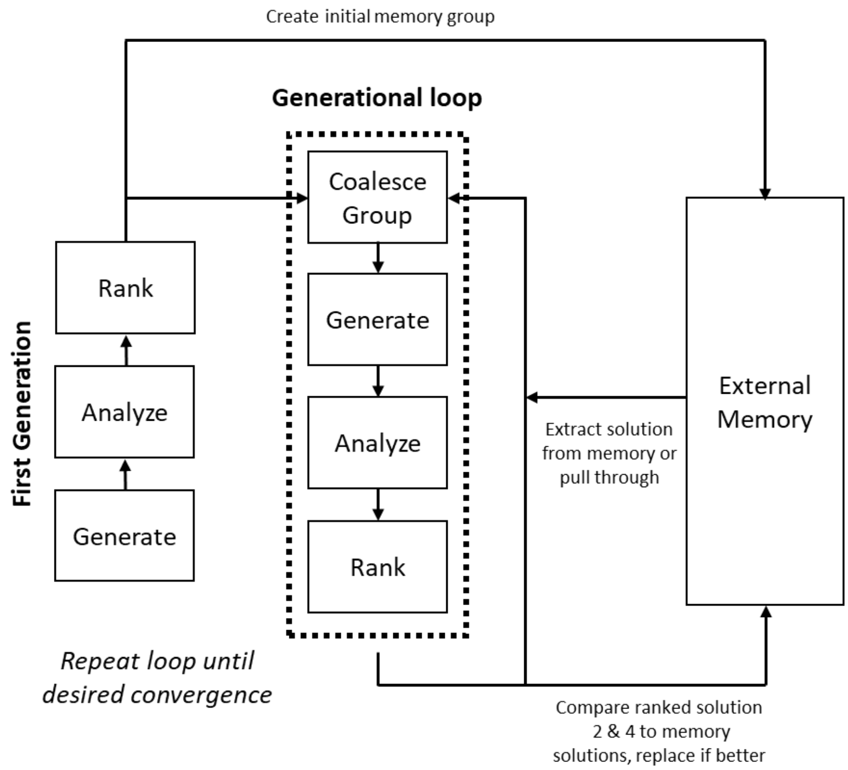

Figure 7: Diagram of the genetic algorithm flow

solution has a lower entropy generation rate than the memory solution, it will be recorded as replacing it in the final memory output. If the memory solution has the lower value, it remains in the memory and its solution array replaces the solution in the current generation. Once the final generation state has been created, the new generation can be created.

The first ranked solution is treated as the elite individual, and thus is not modified in the new generation. For the rest of the solutions, a crossover occurs first, and creates crossovers between 1-2, 2-3, 3-4 and 4-5. When the operator initializes, it copies both parent arrays to its own memory, and initializes the new child using the first parent as a base. Similar to the generation technique, the script runs through each array row by row until it reaches the bottom. At each point, a random number is generated and this determines if the second parent provides the data for that point. There is a 50% chance that the second parent will be used. If a solid pixel will be added to the space, it follows the same rules as point generation. The pixel must have another solid pixel around it, or it will not generate. Deleting a solid pixel is a much more difficult issue, as it is very easy to create geometry that cannot physically exist. For example, if three pixels extend from the edge of a solid part, and you delete the first pixel that starts the extension, the two end pixels will remain in space. To get around this issue, a few filters are used in the system. In this instance, rules are set to determine what can be deleted, similar to the requirements on what can be added. If there are two solid pixels around the current pixel, then the system is not allowed to delete the current position. This is done to prevent the deletion of bridges between shapes. While there is some loss of accuracy, it is a necessary tradeoff to produce realistic designs. In exchange for the increased error, chance of crossover is increased to 60% for bit deletion.

With the crossover operation completed, mutation can be performed. The system goes through each pixel in the array, and will check the mutation percentage (30% for creation, 40% for deletion) against a randomly generated value. If the value is less than the percentage chance, the pixel bit in the current position will be flipped. That is, if it is a solid pixel, it will be changed to empty space, and if it is empty space, it will become a solid pixel. At the same time, the pixel change still must follow the rules laid out previously for both creating a solid pixel, and deleting a pixel. With mutation done, all the algorithms are complete. A filter is now utilized to clear any remaining outliers in the array. The filter is very simple in design and execution; it goes through each locational point and looks at the surrounding pixel count of every solid pixel. If there are 2 or less solid pixels surrounding, the selected solid pixel is deleted. A balance had to be chosen for this filter, as just deleting shapes with only one surrounding pixel will leave a lot of the extraneous shapes in the final array. Any more, and a large amount of valuable information will be lost. In the end, two was selected as it offered a good balance of deleting bad bits, while not sacrificing a large amount of functional data.

With the final arrays created, the new generation information can be exported an analyzed, as described in Section 3. The process is continued until 100 generations have been run, which typically sees complete solution convergence.

4. Results and Discussion

The performance of every generated profile is compared against a standard finned heat sink, which occupies the same overall volume. The finned heat sink has 19 interior fins, 1 mm thick, with a spacing of 1.55 mm between each fin. Again, this is based on the design from Remsburg [9]. The pressure drop of the baseline fin system at a flow rate of 0.1 m/s is calculated as 59.34 Pa. Utilizing the symmetric power map, it is found that the entropy generation rate is 0.2649 W/K. The non-symmetric power map results in the generation rate being 0.02445 W/K, as less heat is transferred. These values serve as the baseline that all generated designs are compared to.

4.1 Symmetric Power Map Results

Before the results are discussed, it should be noted that an error was encountered during the initial generation attempt. This error was from the algorithm not correctly implementing the elitist solution. As a result, the elite solutions were all based off of the first generation best result. It was discovered after 38 generations were completed, so it was decided to seed a new, corrected solution set with the results up to that point. This was done to determine the effects of a strong initial population on the algorithm process. To better determine how quickly the ideal solution may emerge from a typical scenario (i.e., with no strong initial population), the analysis with the non-symmetric power was started with no initial seeding.

After 100 generations, the five lowest entropy generation rates were determined to be 0.1992, 0.2033, 0.2078, 0.2082 and 0.2085 W/K. These geometries are shown in Figure 8. From initial inspection, the largest mass of material is in the center of the cross section, with some extension toward the edge. Mass tends to start at the base center, and then branch out further, conducting heat away from the hottest portion of the chip. The far edge of the device sees less overall mass than the center areas. Most of the open area occurs around the far edge and the top of the device. To quantify, the solutions were subdivided into 5 sections, with the fill in the areas calculated and shown in Figure 9. Sections 2, 3 and 4 represent the center of the device, and it can be noted that the fill densities are consistently within 50-55% for these areas. This is in contrast to the outer edges analyzed by sections 1 and 5, where the fill density is typically closer to 45-

50%. This confirms that the system is biasing solid material toward the center of the devices. Total fill density of the devices was also determined, at 53.97, 50.11, 49.21, 52.15 and 49.21% for the respective solutions.

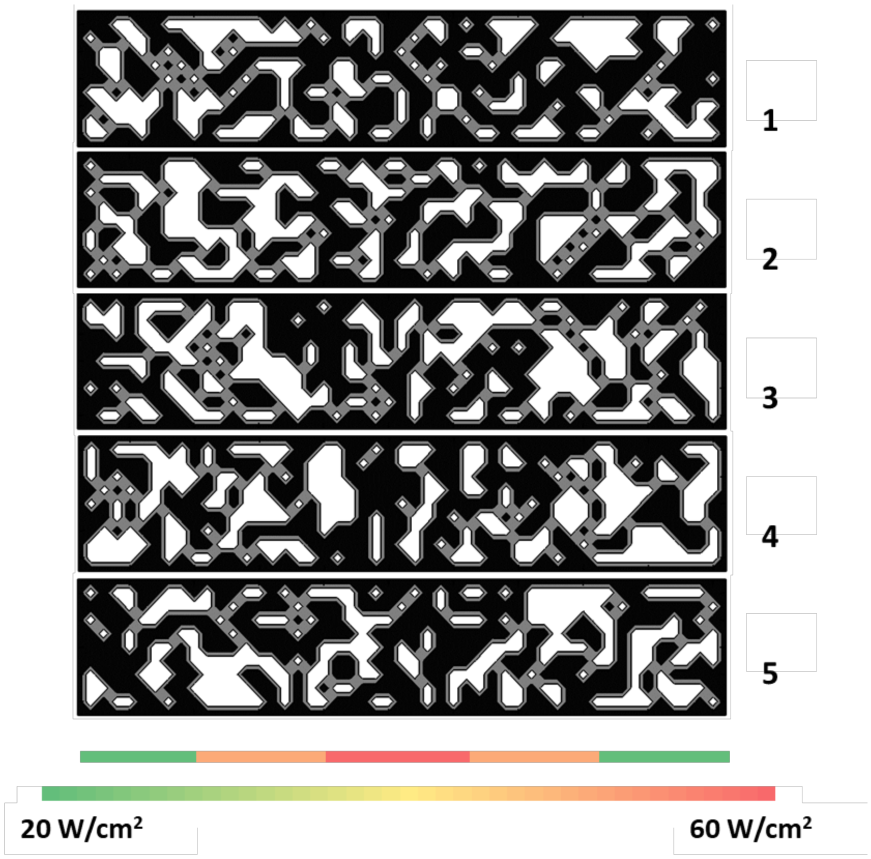

Figure 8: Contour figures of the top five solutions providing the lowest entropy generation rate utilizing the symmetric power profile

Compared to the finned heat sink at 0.2649 W/K, the reduction in entropy generation rate for the optimized solutions was between 21 and 25%. Similarly, these five designs had a reduction in thermal resistance from 24 to 27% compared to the baseline. This also corresponds to a drop in maximum surface temperature of up to 11.27 K. The reduction in thermal resistance is accompanied by an increased pressure drop compared to the fin design (59.43 Pa). The top five generated designs have a pressure drop of 349.0, 261.4, 226.7, 290.4 and 216.0 Pa respectively. This is a respective increase of 487, 340, 281, 389 and 264%. This is a noticeable increase over the finned system, and is best explained by the relative irreversibility due to pressure loss of the working fluid compared to heat transfer over a finite temperature difference. As the pressure drop is on the scale of Pa, a significant change on the order of 100 Pa will not have the same effect as a change of a few Kelvin on the maximum temperature for a fixed heat input. Thus, from a thermodynamic perspective, the overall heat removal process is more reversible in the generated heat sinks, despite the increased pressure drop. However, practically, the thermodynamic improvement would need to be balanced with potentially higher pump operating costs.

It is well established that higher heat transfer coefficients and lower thermal resistance can be obtained by decreasing hydraulic diameters, at the expense of pressure drop. To assess if the observed gains compared to the fin sink were merely due to smaller flow passages, the finned geometry was simulated again with higher inlet velocities to match the pressure drop of top generated results. For the symmetric map solution, inlet velocity was increased to 0.345 m/s compared to 0.1 m/s of the original study. At this higher flow rate, the finned solution entropy generation rate was 0.2376 W/K. This means the entropy generation rate of the generated solution is still 16.9% less, and has a thermal resistance 16.2% lower, indicating that the optimization algorithm and unconstrained manufacturing approach would offer some advantage.

4.2 Non-Symmetric Power Map Results

When utilizing the power map based on the CPU power map (geometry shown in Figure 11), it was found the top five generated solutions had entropy generation rates of 0.01920, 0.01966, 0.02001, 0.02005 and 0.02012 W/K. This is compared to the finned heat sink at 0.02445 W/K, a reduction between 18 and 21%. The reduction in thermal resistance for the generated geometries is between 18 and 22%. Because the difference in overall power is much smaller than the symmetric case, the reduction in maximum temperature is not as significant as the symmetric map solutions, at 2.5 K. Again, this added performance comes at a cost of pressure drop compared to the finned design (59.34 Pa). The top five generated designs have a pressure drop of 328.3, 395.2, 336.9, 289.1 and 302.6 Pa respectively. This is a respective increase of 453, 566, 468, 387 and 410%. As discussed before, this is a noticeable increase compared to the traditional finned system, and thermodynamic improvement from an entropy generation perspective must be weighed against practical issues such as pumping power.

In general, the solutions have the most mass concentrated to the high power regions of the corresponding power map. It is notable that the power is more evenly distributed in the non-symmetric profile, and the effects this has on flow channels. The channels with the non-symmetric map are fairly consistent in diameter and size across the solution space, while the symmetric map sees larger diameter channels on the outer edges where power inputs are lower. Similar to the symmetric study, the finned solution was reran with a higher inlet velocity to match the pressure drop of the top generated solution. This velocity was placed at 0.335 m/s. The entropy generation rate is 0.02056 W/K. The top generated solution entropy generation rate and thermal resistance are still 6.6% less than this new solution. Again, the generated results still show improved performance.

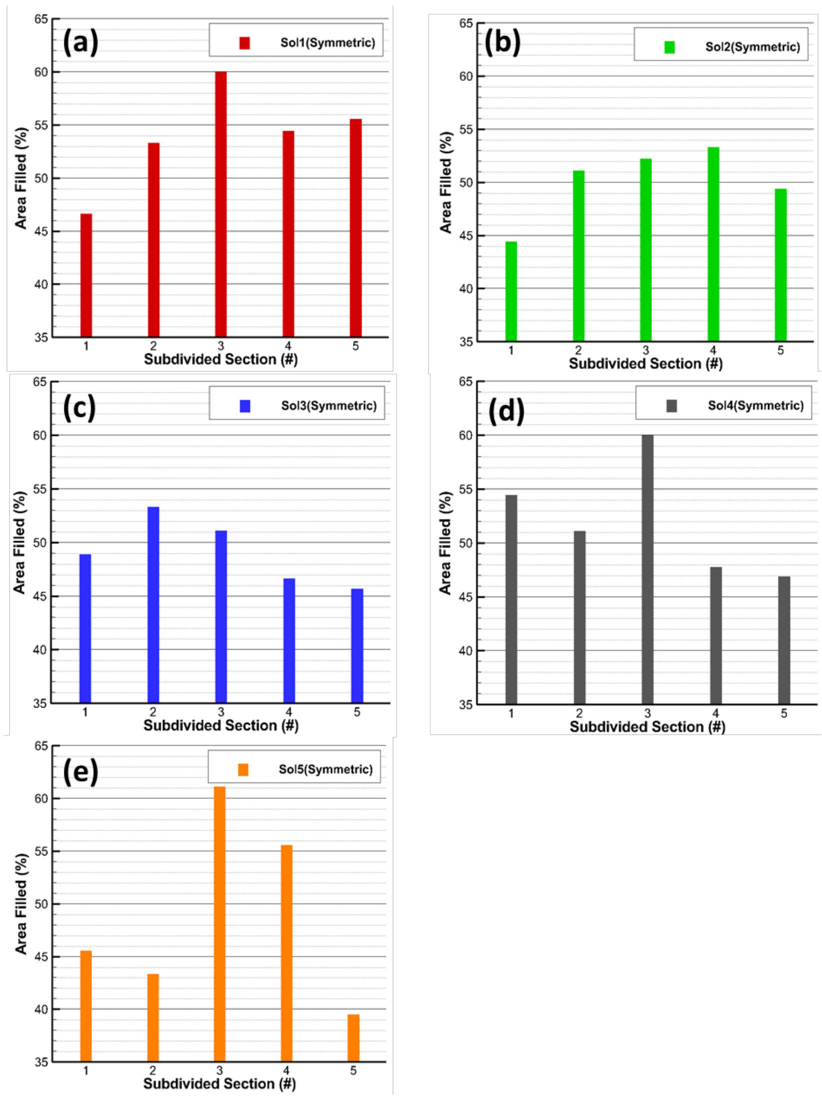

Figure 9: Fill density of top five symmetric solutions

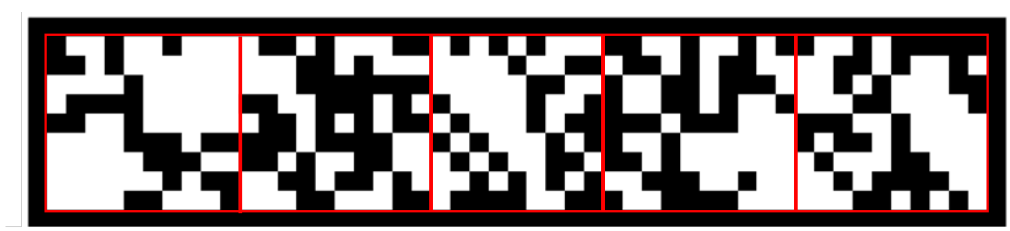

Section: 1 2 3 4 5

Figure 10: Illustration of section division of a solution

4.3. Algorithm Effectiveness

The distribution of solutions is shown in Figure 12 for both power maps. Elite solutions were removed from the data to provide a clearer view on the effects of the algorithm on generated solutions. Note that the solutions are mostly stochastic over the generations, which can be confirmed by examining the generational averages in Figure 13. The averages are characterized by peaks and valleys, similar to those seen by Gagne and Andersen [28] for their single objective optimization analysis. When viewing the minimum value of each generation, however, a logarithmic decrease is notable with the non-symmetric power map solutions. The seeding of the symmetric map does mean the solution is near optimized from the

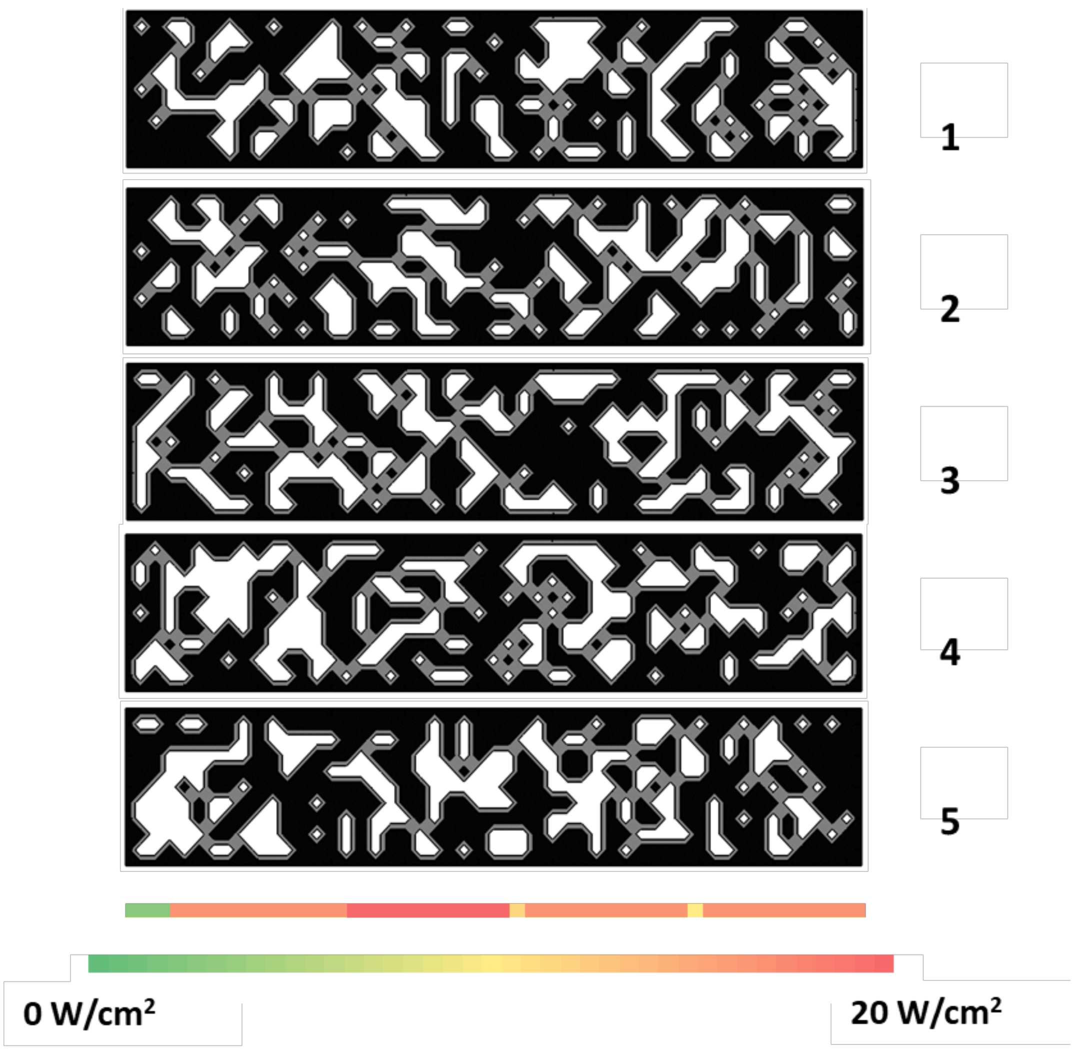

Figure 11: Contour figures of the top five solutions providing the lowest entropy generation rate utilizing the non-symmetric power profile.

beginning of the algorithm, and only sees an improvement after 72 generations. Interestingly, this is slightly slower than the optimum in the non-symmetric, which arrived after 57 generations.

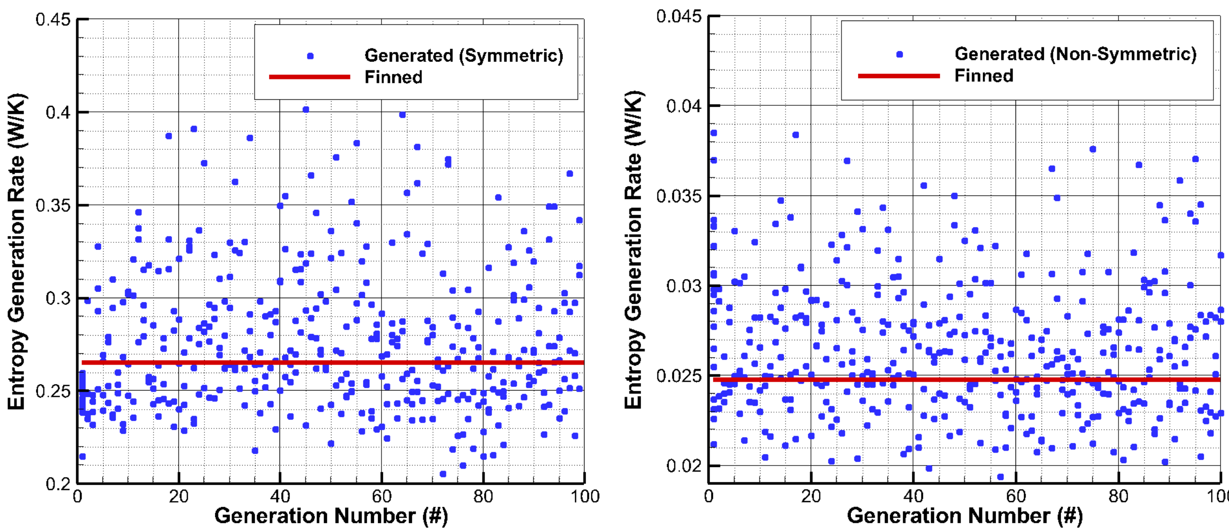

Figure 12: Entropy generation of each solution versus generation number

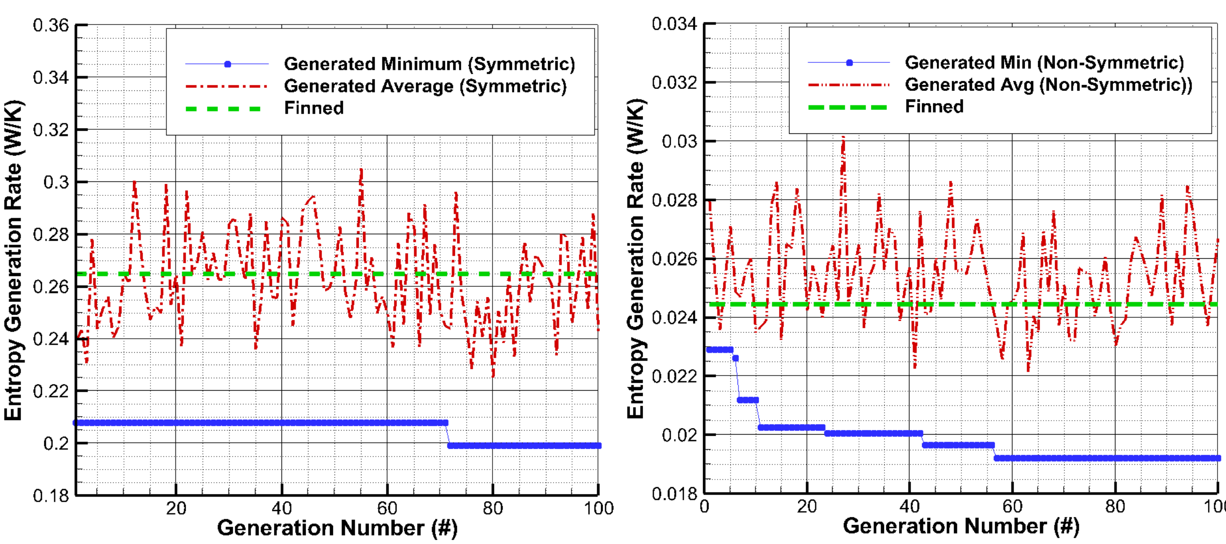

Figure 13: Generation average (without elite solution) and minimum entropy generation rate versus generation number

4.4. Uncertainty

There are a few sources of uncertainty in the analysis. Among them, the potential uncertainty from using a turbulent model compared to a laminar, the grid convergence index, uncertainty in the energy input and round off uncertainty. The turbulent model saw a maximum of 5.3% difference from the laminar model pressure drop. Grid convergence index saw a 0.53% difference in pressure drop between a 1/2 grid step, and 1.33% change in temperature. A maximum of 1% difference in the input power was allowed in the system solution, and is the assumed uncertainty of the energy. Finally, the round-off was set at four decimal places, resulting in a percentage error on the order of 10^{-7}. Using these values, the propagated uncertainty in the entropy generation rate was evaluated for two of the best solutions, two median and two of the worst solutions for each analysis following the guidelines of Taylor and Kuyatt [29].

From this, the total uncertainty of the entropy generation rate ranges between 1.5 to 1.75%. The thermal resistance is approximately 1.75% and the pressure drop is approximately 5.33%. It is an interesting note that the pressure drop has almost no impact on the uncertainty of the entropy generation rate, which is dominated by the base temperature (67% of the total uncertainty) and the energy input (33% of the total uncertainty).

4.5 Study Limitations

A key limitation of the methodology introduced here is the lack of sufficient process automation and long computation time required. Both of these are areas ripe for further research and improvement. As an example, for the first generation of each case study, there were between 20 and 25 different solutions that had to be simulated, whereas each following generation had 5 (although only 4 were new, due to micro-genetic algorithm approach). Using a standard laboratory workstation (Intel Xeon processor with 8 GB of RAM), a simulation of each solution required approximately 3 hours, which led to about 690 hours of simulation time per case study, running two simulations in parallel. This time could be significantly reduced by improving the computational power and/or improving the laminar/turbulence model. In addition, coupling between the different software tools could be automated to minimize user required input.

However, moving to a full 3D optimization will place an even larger demand on computational time and resources. This suggests that investigation of reduced order models that can still provide accurate predictions of heat transfer and pressure drop in unconventional geometries while reducing computational time are of interest. Despite these limitations, the micro-genetic algorithm approach investigated here demonstrates a pathway for integrating more detailed component simulation with a genetic algorithm approach.

5. Conclusion

Results from this study show potential for unrestricted heat sink designs optimized using micro-genetic algorithms and a bit-array representation. The optimized heat sinks were able to decrease entropy generation rate by 25% and 21% for the symmetric and non-symmetric maps respectively compared to a finned system. Additionally, thermal resistance saw a respective decrease by 27% and 22%, but in exchange for greater system pressure drops at an increase of 487% and 453% each. This gain in pressure drop is a result of the use of the entropy generation rate as the guiding metric, which as a result of the small changes in the absolute pressure drop, biased the system toward solutions that greatly reduced the maximum temperature of the input surface.

With a promising baseline established, there are is a need for additional research. Importantly, little effort has been made into the experimental investigation of heat sinks developed through additive manufacturing. On the computational side, while this research focused on modifying the geometry in the frontal X-Y plane, there is also potential of modification along the flow path in the X-Z plane. Ultimately, 3D optimization in the X-Y and X-Z would allow additive manufacturing approaches to be maximally exploited. Achieving this goal requires research on how to minimize computational time, through parallelization and other approaches. In the current study, each analysis took approximately 690 hours to complete. Through changes such as changes to a laminar flow model and improved computing resources, this could be reduced to close to 190 hours. Such improvements could extend into 3D analysis, and bring more reasonable analysis times. Another area that can be expanded upon is that of the optimization algorithm. In this analysis, a multi-objective problem was simplified to that of a single-objective problem by the use of entropy minimization. Expansion of the methods back toward a true multi-object algorithm would allow greater design flexibility, allowing designers to pick and choose what their optimum goals are. Further optimization can be made to the methodology to enable it to become faster and easier to use. This includes steps such as automation of ANSYS Workbench through scripts, as well as the automation of the new solution generation process. Combined with small changes such as the elimination of small gaps resulting from diagonal bits, and modification of the analysis model to utilize laminar flow, uncertainties could be reduced and analysis time greatly improved. Finally, the biggest gap is the lack of experimental research which is necessary to validate the results of this research, and could determine the potential of the technology. The combination of further research and technology advancement could allow the technique to become a viable option for use within industry.

Acknowledgements

This research was supported by Intel® Corporation.

References

[1] K. V. Wong, A. Hernandez, A Review of Additive Manufacturing, ISRN Mech. Eng. 2012 (2012) 1–10. doi:10.5402/2012/208760.

[2] XJet 3D, (2017). https://xjet3d.com.

[3] T. Bauer, K. Dawson, A.B. Spierings, K. Wegener, Microstructure and mechanical characterisation of SLM processed Haynes® 230, J. Chem. Inf. Model. 53 (2013) 1689–1699. doi:10.1017/CBO9781107415324.004.

[4] D. Thomas, S. Gilbert, Costs and Cost Effectiveness of Additive Manufacturing - A Literature Review and Discussion, NIST Spec. Publ. 1176 (2014) 1–77. doi:10.6028/NIST.SP.1176.

[5] C.D. Chapman, K. Saitou, M.J. Jakiela, Genetic Algorithms as an Approach to Configuration and Topology Design, J. Mech. Des. 116 (1994) 1005. doi:10.1115/1.2919480.

[6] S.Y. Wang, K. Tai, Structural topology design optimization using Genetic Algorithms with a bit-array representation, Comput. Methods Appl. Mech. Eng. 194 (2005) 3749–3770. doi:10.1016/j.cma.2004.09.003.

[7] S.Y. Wang, K. Tai, M.Y. Wang, An enhanced genetic algorithm for structural topology optimization, Int. J. Numer. Methods Eng. 65 (2006) 18–44. doi:10.1002/nme.1435.

[8] L. Gosselin, M. Tye-Gingras, F. Mathieu-Potvin, Review of utilization of genetic algorithms in heat

transfer problems, Int. J. Heat Mass Transf. 52 (2009) 2169–2188. doi:10.1016/j.ijheatmasstransfer.2008.11.015.

[9] R. Remsburg, Nonlinear fin patterns keep cold plates cooler, Power Electron. Technol. 33 (2007) 22–27. https://www.scopus.com/inward/record.uri?eid=2-s2.0-33947281868&partnerID=40&md5=b3bc09102bb01f2d649dcb5d75a8de84.

[10] R.C. Eberhart, Y. Shi, Comparison between genetic algorithms and particle swarm optimization, Evol. Program. VII. (1998) 611–616. doi:10.1007/BFb0040812.

[11] M. Gen, R. Cheng, Genetic Algorithms and Engineering Optimization, 1999. doi:10.1002/9780470172261.

[12] K. Deb, S. Agrawal, Understanding interactions among genetic algorithm parameters, Found. Genet. Algorithms V, San Mateo, CA Morgan Kauffman. (1999) 265–286. doi:citeulike-article-id:4372866.

[13] C.A.C. Coello, G.T. Pulido, A Micro-Genetic Algorithm for Multiobjective Optimization, (2001) 126–140.

[14] H.E. Ahmed, B.H. Salman, A.S. Kherbeet, M.I. Ahmed, Optimization of thermal design of heat sinks: A review, Int. J. Heat Mass Transf. 118 (2018) 129–153. doi:10.1016/j.ijheatmasstransfer.2017.10.099.

[15] R. Bornoff, J. Parry, An additive design heatsink geometry topology identification and optimisation algorithm, Annu. IEEE Semicond. Therm. Meas. Manag. Symp. 2015–April (2015) 303–308. doi:10.1109/SEMI-THERM.2015.7100177.

[16] I.K. Karathanassis, E. Papanicolaou, V. Belessiotis, G.C. Bergeles, Multi-objective design optimization of a micro heat sink for Concentrating Photovoltaic/Thermal (CPVT) systems using a genetic algorithm, Appl. Therm. Eng. 59 (2013) 733–744. doi:10.1016/j.applthermaleng.2012.06.034.

[17] H. Shen, X. Jin, F. Zhang, G. Xie, B. Sunden, H. Yan, Computational optimization of counter-flow double-layered microchannel heat sinks subjected to thermal resistance and pumping power, Appl. Therm. Eng. 121 (2017) 180–189. doi:10.1016/j.applthermaleng.2017.04.058.

[18] Y.-T. Yang, S.-C. Lin, Y.-H. Wang, J.-C. Hsu, Numerical simulation and optimization of impingement cooling for rotating and stationary pin–fin heat sinks, Int. J. Heat Fluid Flow. 44 (2013) 383–393. doi:10.1016/j.ijheatfluidflow.2013.07.008.

[19] J. Du, M.-N. Yang, S.-F. Yang, Correlations and optimization of a heat exchanger with offset fins by genetic algorithm combining orthogonal design, Appl. Therm. Eng. 107 (2016) 1091–1103. doi:10.1016/j.applthermaleng.2016.04.074.

[20] K. Foli, T. Okabe, M. Olhofer, Y. Jin, B. Sendhoff, Optimization of micro heat exchanger: CFD, analytical approach and multi-objective evolutionary algorithms, Int. J. Heat Mass Transf. 49 (2006) 1090–1099. doi:10.1016/j.ijheatmasstransfer.2005.08.032.

[21] T. Wu, B. Ozpineci, C. Ayers, Genetic algorithm design of a 3D printed heat sink, 2016 IEEE Appl. Power Electron. Conf. Expo. (2016) 3529–3536. doi:10.1109/APEC.2016.7468376.

[22] A. Bejan, Entropy Generation Through Heat and Fluid Flow, Wiley, New York, NY, 1982.

[23] W. a. Khan, J.R. Culham, M.M. Yovanovich, Optimization of Pin-Fin Heat Sinks in Bypass Flow Using Entropy Generation Minimization Method, J. Electron. Packag. 130 (2008) 031010.

doi:10.1115/1.2965209.

[24] MathWorks, MATLAB, (2015).

[25] ANSYS, Fluent, (2016).

[26] ANSYS, DesignModeler, (2016).

[27] C. Greene, C2xyz contour matrix to coordinates, Mathworks File Exch. (2014). https://www.mathworks.com/matlabcentral/fileexchange/43162-c2xyz-contour-matrix-to-coordinates.

[28] J.M.L. Gagne, M. Andersen, Multi-Objective Facade Optimization for Daylighting using a Genetic Algorithm, IBPSA. 9 (2010) 110–117.

[29] B.N. Taylor, C.E. Kuyatt, Guidelines for Evaluating and Expressing the Uncertainty of NIST Measurement Results - NIST Technical Note 1297, Gaithersburg, MD, 1994.